IEEE Access
Multidisciplinary | Rapid Review | Open Access Journal

Received October 8, 2017, accepted November 15, 2017, date of publication November 29, 2017,
date of current version December 22, 2017.

Digital Object Identifier 10.1109/ACCESS.2017.2778425

Joint Synchronization and Localization for Underwater Sensor Networks Considering Stratification Effect

BINGBING ZHANG, (Student Member, IEEE), HONGYI WANG, LIMING ZHENG, JIANFEI WU, AND ZHAOWEN ZHUANG

School of Electronic Science, National University of Defense Technology, Changsha 410073, China

Corresponding author: Bingbing Zhang (zbbzb@nudt.edu.cn)

This work was supported in part by the Major Research Development Program of Hunan province of China under Grant 2016JC2008, in part by the China Post-Doctoral Science Foundation under Grant 2016T90978, and in part by the National Nature Science Foundation of China under Grant 61604176.

ABSTRACT In underwater wireless sensor networks, time synchronization and localization are basic requirements in many applications. A joint synchronization and localization framework is expected to provide better accuracy. In this paper, we propose a unified framework to execute synchronization and localization simultaneously taking stratification effect into account. In this method, the stratification effect of underwater medium is modeled using a ray tracing approach. The maximum likelihood (ML) estimator is derived, which is shown to be highly nonlinear and nonconvex. Therefore, we employ the Gauss–Newton algorithm to solve the original nonconvex ML problem in an iterative manner. Furthermore, the Cramér–Rao lower bound for this problem is derived as a benchmark. Simulation results indicate that the proposed method outperforms the existing methods in both accuracy and energy efficiency.

INDEX TERMS Underwater sensor networks (UWSNs), synchronization, localization, maximum likelihood (ML), Gauss-Newton method, stratification effect.

I. INTRODUCTION

Nowadays, underwater wireless sensor networks (UWSNs) have received a significant attention in the literature, largely due to their wide range of marine applications, such as ocean environment monitoring, disaster forecasting, assisted navigation, resource exploration and military purposes [1], [2]. Time synchronization and localization are essential services in UWSNs. Since the electromagnetic wave will experience high attenuation in water, acoustic communication is more suitable for UWSNs. The unique characteristics of underwater acoustic channel present great difficulties and challenges to the implementation of time synchronization and localization in UWSNs [3], [4]. For example, depth-dependent sound speed profile (SSP, which defines the sound propagation speed as a function of the ocean depth), high propagation delays, low data rate and narrow communication bandwidth impose more limits on the development of applications based on UWSNs. In addition, the available energy for underwater sensor nodes is very limited, due to the high cost of changing or recharging its battery.

Similar to terrestrial wireless sensor networks (WSNs), UWSNs consist of anchor nodes, whose locations are known and clocks are synchronized, and ordinary nodes with unknown locations whose clocks need to be synchronized. Time synchronization and localization are typically realized by exchanging a sort of messages between the anchor node and the ordinary node. However, they are usually considered separately. Commonly, the original estimation problem is solved by using a two-step approach, where the synchronization is first performed and then the localization is performed. However, this approach can lead to poor accuracy of both synchronization and localization because the two estimation problems are handled independently [5], [6]. Alternatively, a joint synchronization and localization framework is expected to provide better accuracy due to the close relationship between time synchronization and localization [7]. In UWSNs, most of accurate localization methods are based on the time of arrival (TOA) measurements. Their performances rely heavily on the clock synchronization accuracy of the relevant nodes. On the other hand, time synchronization

benefits from the knowledge of location which can be used to estimate propagation delays. Furthermore, the messages exchanged between the ordinary node and anchor nodes bearing both the location and clock information. Thus, the time synchronization and localization tasks can be accomplished based on a single sort of messages. This reduces the message exchanging frequency and consequently saves the energy. Therefore, we believe that to formulate them into a unified framework is beneficial to accuracy improvement and energy conservation.

Among the aforementioned challenging characteristics of underwater synchronization and localization, we are interested in the depth-dependent SSP which varies with temperature, pressure, and salty [8]. Due to this property, the sound waves do not propagation along a straight line in real UWSNs. In contrast, the propagation path bents, and the Euclidean distance between the nodes is not the one that traveled by an acoustic wave. This phenomenon is described as stratification effect [9]. The joint synchronization and localization method for terrestrial WSNs have been investigated recently [7]. However, the stratification effect in underwater environment degrades the effectiveness of these methods. This is mainly because the radio speed is nearly a constant in terrestrial, and thus the radio waves can be considered propagating along a straight line.

Aiming at the stratification effect of underwater environment, in this paper, we propose a joint synchronization and localization algorithm based on Gauss-Newton method for UWSNs, called GN-JSL. In this algorithm, the SSP is assumed to only linearly depend on the depth [10]. The ordinary node to be synchronized and positioned is assumed as a fixed point during the message exchange process. Using ray tracing method to model the stratification effect is first introduced. Then, the stratification effect, clock drifts and ordinary node's location are formulated into a unified framework. The corresponding maximum likelihood (ML) estimator is derived which is shown to be highly nonlinear and nonconvex. The Gauss-Newton algorithm is employed to solve the original nonconvex ML problem in an iterative manner. To compare different approaches, the Cramer-Rao lower bound (CRLB) for this problem is derived as a benchmark. Simulation results indicate that the proposed method outperforms the existing methods in both accuracy and energy efficiency.

The remainder of the paper is organized as follows. In section II, we first review the related work on time synchronization and localization methods in UWSNs. Section III explains the system model considered in this paper. In section IV, we describe the GN-JSL method in detail. Section V evaluates the performance of the proposed method through several simulations, and section VI concludes the paper.

II. RELATED WORKS

A complete survey of studies on time synchronization for terrestrial WSNs can be found in [11]. There are some widely-used time synchronization protocols, such as reference broadcast synchronization (RBS) [12], timing-sync protocol for sensor networks (TPSN) [13], light-weight time synchronization (LTS) [14], and flooding time synchronization protocol (FTSP) [15]. However, these algorithms appear to be less effective in UWSNs for several reasons. Firstly, most of them assume the propagation delays among sensor nodes are negligible. This is reasonable for radio communication due to the high speed of electromagnetic waves. For UWSNs, on the contrary, the low propagation speed of acoustic channel (about 1500 m/s) results in longer propagation delay which is non-ignorable. Secondly, the energy efficiency of terrestrial time synchronization algorithms is not considered generally. In contrast, due to the limited capacity of underwater sensor's battery, the UWSNs need to be energy efficient. Moreover, all the time synchronization algorithms designed for terrestrial WSNs can not tackle the stratification effect in UWSNs, which will severely worsen the synchronization accuracy.

In the literature, some time synchronization algorithms for UWSNs have been proposed, including TSHL [16], MU-Sync [17], D-Sync [18], Mobi-Sync [19], and DA-Sync [20]. These algorithms mainly focused on the compensation for long propagation delays and sensor nodes' mobility to improve the synchronization accuracy and energy efficiency. However, the clock synchronization problem is inherently related to the propagation paths of acoustic waves, due to the propagation delay estimation depends on the propagation path. The lack of consideration in propagation model degrades the performance of the previously proposed underwater synchronization algorithms.

There are various localization algorithms already proposed for UWSNs [21]. The work of [21] is a comprehensive survey of localization algorithms for UWSNs. The authors divide localization algorithms into three categories based on the sensor nodes' mobility: stationary localization algorithms, mobile localization algorithms and hybrid algorithms. These algorithms have their own strengths in UWSNs, but all of them can not handle the stratification effect as they assume constant propagation sound speed in underwater environments. Researchers have also proposed some UWSNs localization algorithms with consideration of the stratification effect [22]–[25]. Their localization accuracy is improved by compensating for the non-straight-line propagation model. However, these algorithms are TOA-based, which usually suffer from the clock imperfections. Therefore, the time synchronization among nodes is required.

Tian *et al.* [26] proposed a joint synchronization and localization scheme for UWSNs. In this scheme, the 3D space is partitioned into the shape of truncated octahedrons first, and then the atomic multilateration and iterative multilateration method are employed to obtain the sensor node's clock offset and coordinates. However, this algorithm is not taking into account the clock skew during the synchronization procedure, which severely limits its synchronization accuracy and in turn affects the localization accuracy. In addition, the stratification

effect of water medium is ignored. Diamant and Lampe [27] described a sequential algorithm for joint time synchronization and localization for underwater networks (STSL). STSL takes into account the anchor and ordinary node mobility as well as the sound speed uncertainty. As a result, the localization accuracy of STSL is improved in the presence of time asynchrony and propagation speed uncertainty for a dynamic underwater environment. However, STSL is not considering the stratification effect of water medium, which reduces the accuracy of localization. The most recent work, [28] suggested to jointly synchronize and localize nodes with stratification compensation, and a joint solution is proposed (JSL). JSL is a four phases scheme, which are data collection and rough position estimation, synchronization, localization and iteration. To the best of our knowledge, JSL is the first joint localization and time synchronization scheme, where the stratification effect of underwater medium is considered. However, the time synchronization and localization are performed at different phases, strictly speaking, JSL cannot be categorized as a joint solution. On this basis, we believe that a unified framework as well as the compensation for the stratification effect will further improve the accuracy of time synchronization and localization in UWSNs.

III. SYSTEM MODEL

The main challenges considered in this work are the stratification effect of water medium and the unsynchronized clocks between the ordinary node and anchor nodes, which severely degrade the performance of the previously proposed localization algorithms in UWSNs. In this section, we first review the method of tracing a ray between two nodes to model the stratification effect in underwater environment [25]. Then, the clock model and time of arrival (TOA) measurement model considered in this paper are described.

A. RAY TRAJECTORY

We assume that the underwater SSP is only depth dependent, which can be formulated as:

$$v(z) = az + b, \tag{1}$$

where z denotes the depth, a is the steepness of SSP, and b represents the sound speed at the water surface. The UWSN is three-dimensional, the ray equations are established in a two-dimensional plane which includes both nodes and the z axis. This is because of the cylindrical symmetry property of cylindrical coordinate system, as illustrated in Fig. 1. Let $[x_A, y_A, z_A]^T$ and $[x_B, y_B, z_B]^T$ denote the position of the receiver and sender respectively, where $[\cdot]^T$ denotes matrix transpose. Acoustic propagation is usually treated with a ray-theory approach which is a valid approximation for underwater environment. Ray tracing method is guided by the Snell's law [23]:

$$\frac{\cos\theta}{v(z)} = \frac{\cos\theta_A}{v(z_A)} = \frac{\cos\theta_B}{v(z_B)} = k, \quad \text{and } \theta_A, \theta_B \in [-\frac{\pi}{2}, \frac{\pi}{2}] \tag{2}$$

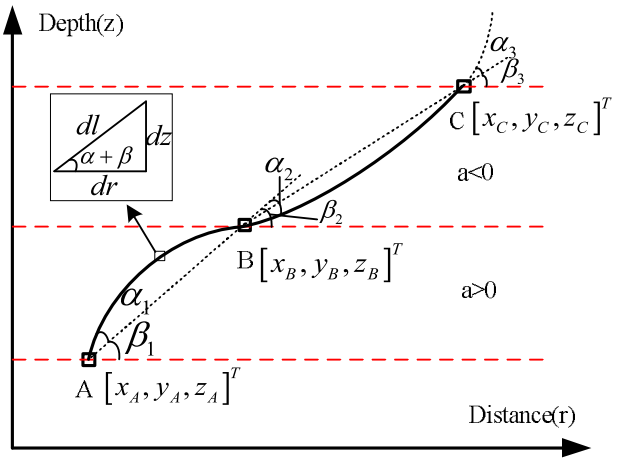

FIGURE 1. Illustration of the stratification effect.

where $\theta_A = \beta_1 + \alpha_1$ and $\theta_B = \beta_2 - \alpha_2$, which are the ray angles at the receiver and the sender locations, respectively. From Fig. 1, we can obtain that $\beta_1 = \beta_2$ and $\alpha_1 = \alpha_2$ due to the symmetry of the arc. z_A and z_B denote the depth of the receiver and the sender respectively, and k is a constant associated with the water medium. Without loss of generality, the parameters θ and z represent the angle and the depth of a given point on the ray trajectory. As illustrated in Fig. 1, a set of differential equations can be written as follows:

$$dr = \frac{dz}{\tan\theta}, \quad dl = \frac{dz}{\sin\theta}, \quad dt = \frac{dl}{v(z)}, \tag{3}$$

where l is the arc length of acoustic propagation path between the two nodes. The notation r denotes the horizontal distance between the sender and receiver, can be represented as:

$$r = \sqrt{(x_B - x_A)^2 + (y_B - y_A)^2}, \tag{4}$$

Finally, the propagation delay between the sender and the receiver can be calculated as (for further details see [25]):

$$X = \frac{z_B - z_A}{r} \tag{5a}$$

$$K = \frac{0.5a(z_B - z_A)}{b + 0.5a(z_B + z_A)} \tag{5b}$$

$$Y = \begin{cases} \dfrac{K}{X} & z_A \neq z_B \\ \dfrac{0.5ar}{b + az_A} & z_A = z_B \end{cases} \tag{5c}$$

$$\tan\beta_{i=1,2} = X \tag{5d}$$

$$\tan\alpha_{i=1,2} = Y \tag{5e}$$

$$t = -\frac{1}{a}(\ln\frac{1+\sin\theta_B}{\cos\theta_B} - \ln\frac{1+\sin\theta_A}{\cos\theta_A}), \tag{5f}$$

The analytical results (5a-5f) determine the ray propagation path of two arbitrary nodes in underwater environment. The propagation delay affected by the stratification effect can be calculated using (5f), which is quite different from the straight line model. We will incorporate this stratification effect model into the GN-JSL algorithm.

B. PAIRWISE SYNCHRONIZATION AND LOCALIZATION

Consider a three-dimensional network with N anchors which are located at known positions $\mathbf{s}_i = [x_i, y_i, z_i]^T, i = 1, 2, \ldots, N$, and one ordinary node which is placed at unknown position $\mathbf{x} = [x, y, z]^T$. It is assumed that the anchor nodes are synchronized with a reference clock while the clock of the ordinary node is left to be unsynchronized. The clock of ordinary node can be modeled as a function of the reference clock as:

$$T = \alpha t + \beta, \tag{6}$$

where T and t represent the local time of ordinary node and the reference time, respectively. The parameters α and β denote the clock skew and clock offset, respectively. By estimation the clock skew and clock offset, we can perform time synchronization for pairs of clocks.

In an asynchronous network, joint synchronization and localization requires that the clock parameters and location of the ordinary node must be determined simultaneously from a series of noisy TOA measurements collected within the network. There are two well-known timing message signaling approaches for time synchronization and localization in WSNs: two-way message exchanges and one-way message dissemination. In the former, both anchor and ordinary nodes transmit timing messages. Since acoustic modems typically consume much more power (order of tens of Watts) in transmit mode compared to receive mode (order of milliwatts), the two-way message exchanges is less efficient compared to the one-way message dissemination. In which, either the anchor node or the ordinary node transmits the timing messages, as shown in Fig. 2. For the purpose of improving the energy efficient, one-way message dissemination is adopted in GN-JSL.

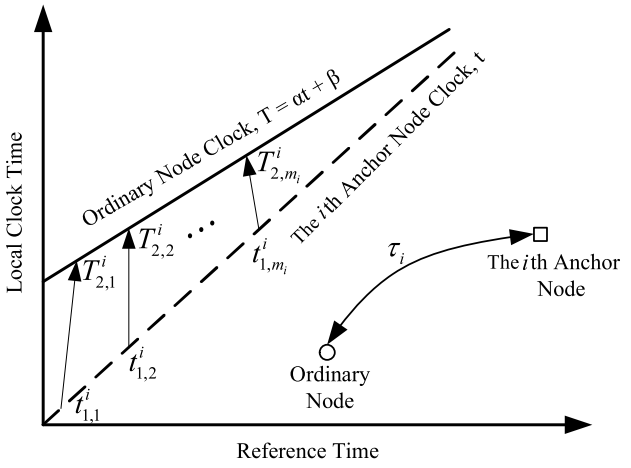

FIGURE 2. Timing messages between the anchor node and ordinary node in one-way approach.

Assume that the anchor nodes are able to stamp the sending time obtained at MAC layer, right before the message leaves. Similarly, the ordinary node is able to stamp the MAC layer time right after the message arrivals. Suppose that the ith anchor node sends its packet at the time stamp $t^i_{1,k}$. This packet includes the current location of the ith anchor node and the time stamp $t^i_{1,k}$. The ordinary node receives the packet at the time stamp $T^i_{2,k}$. Time stamps $t^i_{1,k}$ and $T^i_{2,k}$ are reported based on the local clock of the ith anchor node and the ordinary node, respectively. The measured time stamps at the ordinary node are modeled as:

$$T^i_{2,k} = \alpha(t^i_{1,k} + \tau_i + n^i_k) + \beta, \quad i = 1, \ldots N, \quad k = 1, \ldots, m_i. \tag{7}$$

where τ_i is the propagation delay between the ordinary node and the ith anchor node, which is modeled by (5f). The term n^i_k represents the propagation delay estimation error. The estimation error is modeled as independent and identically distributed (i.i.d.) Gaussian random variable with variance σ^2. The term m_i is the number of packets transmitted by the ith anchor node and successfully received by the ordinary node. It is also assumed that the clock parameters of the ordinary node are fixed during the message exchange phase. Based on the measured time stamps $\{t^i_{1,k}, T^i_{2,k}\}$, one can estimates the location and clock parameters of the ordinary node.

IV. GN-JSL METHOD

The essence of the proposed GN-JSL method is a ML estimator. Thus, in this section, we first derive the ML estimator for the joint time synchronization and localization problem based on the measured time stamps. In the sequel the CRLB of this problem is derived for the CRLB expresses a lower bound on the variance of any unbiased estimator. Then we describe the GN-JSL method in detail.

A. MAXIMUM LIKELIHOOD ESTIMATOR (MLE) AND CRAMÉR-RAO LOWER BOUND (CRLB)

Based on the measurement model in (7), the likelihood function is:

$$p(\mathbf{T}; \mathbf{x}, \alpha, \beta) = \frac{1}{(2\pi\sigma^2)^{L/2}} \exp[-\frac{1}{2\sigma^2}\|\mathbf{T} - \mathbf{f}(\mathbf{x}, \alpha, \beta)\|^2], \tag{8}$$

where $\mathbf{T} = [T^1_{2,1}, \ldots, T^1_{2,m_1}, \ldots, T^i_{2,1}, \ldots, T^i_{2,m_i}, \ldots, T^N_{2,1}, \ldots, T^N_{2,m_N}]^T$, $m_1 + \ldots + m_N = L$, is the vector of measurements and $\|\cdot\|$ is the 2-norm. $\mathbf{f}(\mathbf{x}, \alpha, \beta)$ is a function relating the measured time stamps to the ordinary node's location $\mathbf{x}$ and clock parameters α, β, and it can be represent as:

$$\mathbf{f}(\mathbf{x}, \alpha, \beta) = [(\mathbf{h}^1_{m_1})^T, \ldots, (\mathbf{h}^i_{m_i})^T, \ldots, (\mathbf{h}^N_{m_N})^T]^T, \tag{9}$$

where $\mathbf{h}^m_n = [\alpha(t^m_{1,1} + \tau_m) + \beta, \ldots, \alpha(t^m_{1,n} + \tau_m) + \beta]^T$. Let $\mathbf{u} = [\mathbf{x}^T, \alpha, \beta]^T$ be the vector of the unknown parameters to be estimated, the ML solution of $\mathbf{u}$ is then defined as:

$$\hat{\mathbf{u}}_{ML} = \arg\max_{\mathbf{u}\in\mathbb{R}^5} p(\mathbf{T}; \mathbf{u}), \tag{10}$$

where $\mathbb{R}^5$ represents the 5-dimensional field of real numbers. As observed from (10), the ML estimation problem is highly nonconvex, and therefore it is difficult to solve it analytically.

Thus, we utilize the Gauss-Newton method to solve the ML estimation problem in an iterative manner. Before the detailed description for the proposed algorithm, the CRLB is derived first in order to provide the performance benchmark.

Recall from (7) that the vector of measurements $\mathbf{T}$ is modeled as a Gaussian random vector:

$$\mathbf{T} \sim \mathcal{N}(\mathbf{f}(\mathbf{u}), \mathbf{C}), \tag{11}$$

where $\mathbf{C} = (\alpha\sigma)^2\mathbf{I}_L$, $\mathbf{I}_L$ denotes the $L \times L$ identity matrix. The elements of the Fisher information matrix (FIM) can be obtained as [29]:

$$[\mathbf{J}(\mathbf{u})]_{i,j} = [\frac{\partial \mathbf{f}(\mathbf{u})}{\partial [\mathbf{u}]_i}]^T \mathbf{C}^{-1} [\frac{\partial \mathbf{f}(\mathbf{u})}{\partial [\mathbf{u}]_j}]^T + \frac{1}{2} tr[\mathbf{C}^{-1} \frac{\partial \mathbf{C}}{\partial [\mathbf{u}]_i} \mathbf{C}^{-1} \frac{\partial \mathbf{C}}{\partial [\mathbf{u}]_j}], \quad i,j = 1,2,3,4,5 \tag{12}$$

where $[\cdot]_{i,j}$ stands for the (i,j)th element of the matrix, $[\cdot]_i$ stands for the ith element of the vector, $tr[\cdot]$ stands for the trace of the matrix. From (9), $\frac{\partial \mathbf{f}(\mathbf{x},\alpha,\beta)}{\partial [\mathbf{u}]_i}$ can be obtained as follows:

$$[\frac{\partial \mathbf{f}(\mathbf{u})}{\partial [\mathbf{u}]_i}]_k = \begin{cases} \alpha \frac{\partial \tau_k}{\partial x}, & if\ i = 1 \\ \alpha \frac{\partial \tau_k}{\partial y}, & if\ i = 2 \\ \alpha \frac{\partial \tau_k}{\partial z}, & if\ i = 3 \\ t_{1,k} + \tau_k, & if\ i = 4 \\ 1, & if\ i = 5, \end{cases} \quad k = 1, \ldots, L \tag{13}$$

where τ_k and $t_{1,k}$ denote the propagation delay and the anchor node's time stamp of the kth packet, respectively. Similarly, $\frac{\partial \mathbf{C}}{\partial [\mathbf{u}]_i}$ is given by:

$$\frac{\partial \mathbf{C}}{\partial [\mathbf{u}]_i} = \begin{cases} diag(\underbrace{2\alpha\sigma^2, \ldots, 2\alpha\sigma^2}_{Ltimes}), & if\ i = 4 \\ 0, & otherwise. \end{cases} \tag{14}$$

In order to calculate (13), the derivative of the propagation delay with respect to (w.r.t.) the ordinary node position need to be computed. According to (5f), these partial derivatives can be computed as [25]:

$$\frac{\partial \tau_k}{\partial x} = -\frac{\alpha}{a}(\frac{1}{\cos\theta_{\mathbf{x},k}} \frac{\partial \theta_{\mathbf{x},k}}{\partial r} - \frac{1}{\cos\theta_{\mathbf{s}_{\mathbf{i},k}}} \frac{\partial \theta_{\mathbf{s}_{\mathbf{i},k}}}{\partial r}) \frac{\partial r}{\partial x}, \tag{15a}$$

$$\frac{\partial \tau_k}{\partial y} = -\frac{\alpha}{a}(\frac{1}{\cos\theta_{\mathbf{x},k}} \frac{\partial \theta_{\mathbf{x},k}}{\partial r} - \frac{1}{\cos\theta_{\mathbf{s}_{\mathbf{i},k}}} \frac{\partial \theta_{\mathbf{s}_{\mathbf{i},k}}}{\partial r}) \frac{\partial r}{\partial y}, \tag{15b}$$

$$\frac{\partial \tau_k}{\partial z} = -\frac{\alpha}{a}(\frac{1}{\cos\theta_{\mathbf{x},k}} \frac{\partial \theta_{\mathbf{x},k}}{\partial z} - \frac{1}{\cos\theta_{\mathbf{s}_{\mathbf{i},k}}} \frac{\partial \theta_{\mathbf{s}_{\mathbf{i},k}}}{\partial z}), \tag{15c}$$

where $\theta_{\mathbf{x},k}$ and $\theta_{\mathbf{s}_{\mathbf{i},k}}$ are the angles at the ordinary node and the anchor node locations of the kth packet, respectively, $x_{i,k}$ and $y_{i,k}$ are the anchor node's x coordinate and y coordinate, respectively. Applying the change of node coordinate values $x_B = x$, $y_B = y$, $x_A = x_{i,k}$ and $y_A = y_{i,k}$, (4) can be modified to $r = \sqrt{(x - x_{i,k})^2 + (y - y_{i,k})^2}$, then, $\frac{\partial r}{\partial x}$ and $\frac{\partial r}{\partial y}$ can be derived as $\frac{x - x_{i,k}}{r}$ and $\frac{y - y_{i,k}}{r}$, respectively. Furthermore, $\frac{\partial \theta_{\mathbf{x},k}}{\partial r}$, $\frac{\partial \theta_{\mathbf{s}_{\mathbf{i},k}}}{\partial r}$, $\frac{\partial \theta_{\mathbf{x},k}}{\partial z}$ and $\frac{\partial \theta_{\mathbf{s}_{\mathbf{i},k}}}{\partial z}$ are given by:

$$\frac{\partial \theta_{\mathbf{x},k}}{\partial r} = \frac{-F_1 F_2}{1 - F_2} \tag{16a}$$

$$\frac{\partial \theta_{\mathbf{s}_{\mathbf{i},k}}}{\partial r} = \frac{F_1}{1 - F_2} \tag{16b}$$

$$\frac{\partial \theta_{\mathbf{x},k}}{\partial z} = \frac{F_4 - F_2 F_3}{1 - F_2} \tag{16c}$$

$$\frac{\partial \theta_{\mathbf{s}_{\mathbf{i},k}}}{\partial z} = \frac{F_3 - F_4}{1 - F_2} \tag{16d}$$

where F_i, $i = 1, 2, 3, 4$ are temporary parameters for display clarity, which are shown as follows:

$$F_1 = -\frac{z - z_{i,k}}{r^2} \frac{(\sin\theta_{\mathbf{x},k} - \sin\theta_{\mathbf{s}_{i,k}})^2}{1 - \cos(\theta_{\mathbf{x},k} - \theta_{\mathbf{s}_{i,k}})} \tag{17a}$$

$$F_2 = -\frac{az + b}{az_{i,k} + b} \frac{\sin\theta_{\mathbf{s}_{i,k}}}{\sin\theta_{\mathbf{x},k}} \tag{17b}$$

$$F_3 = \frac{1}{r} \frac{(\sin\theta_{\mathbf{x},k} - \sin\theta_{\mathbf{s}_{i,k}})^2}{1 - \cos(\theta_{\mathbf{x},k} - \theta_{\mathbf{s}_{i,k}})} \tag{17c}$$

$$F_4 = -\frac{a}{az_{i,k} + b} \frac{\cos\theta_{\mathbf{s}_{i,k}}}{\sin\theta_{\mathbf{x},k}} \tag{17d}$$

where $z_{i,k}$ is the anchor node's z coordinate of the kth packet. Once the FIM is computed, the lower bounds on the error variances for any unbiased estimates of the position and the clock parameters can be computed as:

$$E\{\|\hat{\mathbf{x}} - \mathbf{x}\|^2\} \geq \sum_{i=1}^{3} [\mathbf{J}^{-1}]_{i,i} \tag{18}$$

$$E\{\|\hat{\alpha} - \alpha\|^2\} \geq [\mathbf{J}^{-1}]_{4,4} \tag{19}$$

$$E\{\|\hat{\beta} - \beta\|^2\} \geq [\mathbf{J}^{-1}]_{5,5} \tag{20}$$

B. THE GAUSS-NEWTON METHOD BASED SOLVER

In order to solve the ML estimation problem formulated in (10) using the Gauss-Newton method, we need a suitable initial position that is sufficiently close to the optimal solution. In this paper, the initial position is provided using liner regression. After the message exchange phase, the ordinary node firstly estimates its initial position, which is a coarse position due to the presence of clock imperfections and the stratification effect.

At this stage, we first assume the ordinary node has been synchronized and the sound speed in underwater environment is a constant value. Denote d_k as the corresponding distance for τ_k, and $[x_k, y_k, z_k]^T$ as the position of the anchor node corresponding to the kth packet. Then, we obtain the following equations:

$$d_k^2 = (x - x_k)^2 + (y - y_k)^2 + (z - z_k)^2, \quad k = 1, \ldots, L \tag{21}$$

$$d_k^2 = (c\tau_k)^2, \tag{22}$$

where τ_k can be calculated from (7) with $\alpha = 1$ and $\beta = 0$, and c is the average underwater constant sound speed, which

can be selected from empirical values. In order to using linear least square to solve the problem, an elimination method is utilized to transform (21), which leads to:

$$d_k^2 - d_1^2 = (x_k^2 - x^2) + (y_k^2 - y^2) + (z_k^2 - z^2) - 2(x_k - x)x - 2(y_k - y)y - 2(z_k - z)z. \quad (23)$$

The least squares (LS) estimate of the ordinary node's initial position is given by:

$$\hat{\mathbf{x}}_0 = (\mathbf{A}^T\mathbf{A})^{-1}\mathbf{A}^T\mathbf{B}, \quad (24)$$

where $\hat{\mathbf{x}}_0 = [x_0, y_0, z_0]^T$,

$$\mathbf{A} = \begin{bmatrix} 2(x_2 - x_1) & 2(y_2 - y_1) & 2(z_2 - z_1) \\ 2(x_3 - x_1) & 2(y_3 - y_1) & 2(z_3 - z_1) \\ \vdots & \vdots & \vdots \\ 2(x_k - x_1) & 2(y_k - y_1) & 2(z_k - z_1) \end{bmatrix}, \quad (25)$$

$$\mathbf{B} = \begin{bmatrix} (x_2^2 - {x_1}^2) + (y_2^2 - {y_1}^2) + (z_2^2 - {z_1}^2) - d_2^2 + d_1^2 \\ (x_3^2 - {x_1}^2) + (y_3^2 - {y_1}^2) + (z_3^2 - {z_1}^2) - d_3^2 + d_1^2 \\ \vdots \\ (x_k^2 - {x_1}^2) + (y_k^2 - {y_1}^2) + (z_k^2 - {z_1}^2) - d_k^2 + d_1^2 \end{bmatrix}. \quad (26)$$

The clock skew and clock offset can be expressed as $\alpha = 1 + \delta_\alpha$ and $\beta = 0 + \delta_\beta$, respectively. δ_α and δ_β are small values. This is a reasonable model since the deviation of the clock parameters from the ideal value of $\alpha = 1$ and $\beta = 0$ is not significant for most practical clocks. Thus the initial point for GN-JSL is given by:

$$\mathbf{u}^{(0)} = [x_0, y_0, z_0, 1, 0]^T. \quad (27)$$

Then, the process of the iteration of GN-JSL method can be represented as:

$$\mathbf{u}^{(k+1)} = \mathbf{u}^{(k)} + (\mathbf{H}^T(\mathbf{u}^{(k)})\mathbf{H}(\mathbf{u}^{(k)}))^{-1}\mathbf{H}^T(\mathbf{u}^{(k)})(\mathbf{T} - \mathbf{f}(\mathbf{u}^{(k)})), \quad (28)$$

where $\mathbf{u}^{(k)}$ represents the estimated vector of the unknown parameters attained by the kth iteration. $\mathbf{H}(\mathbf{u}^{(k)})$ can be achieved according to (13) as:

$$[\mathbf{H}(\mathbf{u}^{(k)})]_{i,j} = [\frac{\partial \mathbf{f}(\mathbf{u}^{(k)})}{\partial [\mathbf{u}^{(k)}]_j}]_i. \quad (29)$$

The flow chart of GN-JSL method is shown in Fig. 3. The results in (27) is used to initialize the iteration to improve the rate of convergence. The parameter K denotes the user-defined iteration number, and ε is the threshold of accuracy of the estimate. The iteration goes on until the following condition is satisfied:

$$k > K \ or \ \left\| \mathbf{u}^{(k+1)} - \mathbf{u}^{(k)} \right\| < \varepsilon. \quad (30)$$

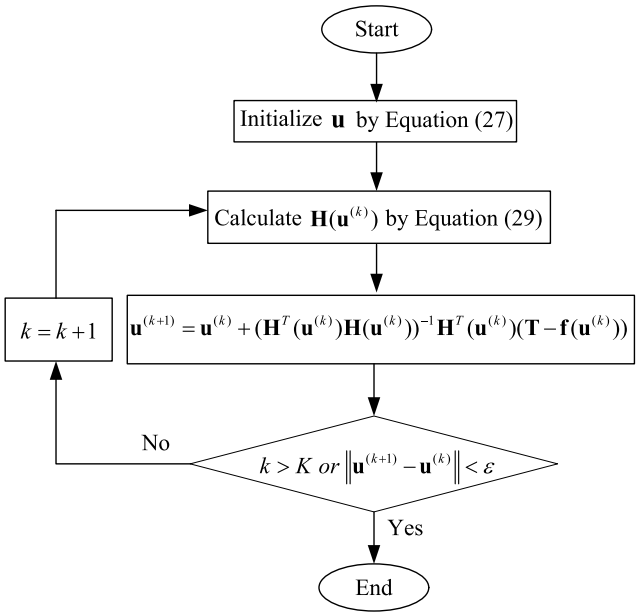

FIGURE 3. Flow chart of GN-JSL.

C. COMPLEXITY ANALYSIS

The complexity of the GN-JSL method is evaluated by the total number of the floating-point operations or *flops*, which is typically a polynomial of the problem dimensions [30]. It is assumed that an addition, substraction, multiplication, division, or square root operation in the real domain can be calculated by one flop. To simplify the expression, the lower-order terms of the complexity expressions are ignored.

To compute the complexity of the estimation of the initial position according to (24), we note that 26 flops are needed to compute a propagation delay based on (5). Then the complexity of the initialization can be obtained as:

$$\begin{aligned} &\text{Flops of LS in (24)} \\ &\simeq \underbrace{6(L-1)}_{\text{cost of computing } \mathbf{A}} + \underbrace{9(2L-3)}_{\text{cost of computing } \mathbf{A}^T\mathbf{A}} \\ &\quad + \underbrace{27}_{\text{cost of computing } (\mathbf{A}^T\mathbf{A})^{-1}} + \underbrace{69(L-1)}_{\text{cost of computing } \mathbf{B}} \\ &\quad + \underbrace{3(2L-3)}_{\text{cost of computing } \mathbf{A}^T\mathbf{B}} \\ &\quad + \underbrace{15}_{\text{cost of computing } (\mathbf{A}^T\mathbf{A})^{-1}\mathbf{A}^T\mathbf{B}}. \end{aligned}$$

In a similar way, the total number of the flops in each loop of the Gauss-Newton iteration can be computed as:

$$\begin{aligned} &\text{Flops of each loop in GN - JSL} \\ &\simeq \underbrace{113L}_{\text{cost of computing } \mathbf{H}(\mathbf{u}^{(k)})} \\ &\quad + \underbrace{L}_{cost\ of\ computing\ (T - f(u^{(k)}))} + \underbrace{25(2L-1)}_{cost\ of\ computing\ H^T(u^{(k)})H(u^{(k)})} \end{aligned}$$

$$+ \underbrace{125}_{\text{cost of computing } (H^T(u^{(k)})H(u^{(k)}))^{-1}} + \underbrace{5(2L-1)}_{\text{cost of computing } H^T(u^{(k)})(T-f(u^{(k)}))} + \underbrace{45}_{\text{cost of computing } (H^T(u^{(k)})H(u^{(k)}))^{-1}H^T(u^{(k)})(T-f(u^{(k)}))} + \underbrace{1}_{\text{cost of computing } u^{(k)}+(H^T(u^{(k)})H(u^{(k)}))^{-1}H^T(u^{(k)})(T-f(u^{(k)}))} + \underbrace{15}_{\text{cost of computing the stopping criteria}}.$$

Then the complexity of the GN-JSL can be approximated as $O(I_{GN-JSL}L)$, where I_{GN-JSL} is the number of iterations in the GN-JSL method to converge to the solution. To compare the complexities, we have also measured the average computational time of different methods for a cubic network with edge length 2000 m and 8 anchor nodes as considered in Section V. The algorithms are implemented in MATLAB R2013a on a HP ProDesk 480 (Processor 3.3 GHz Intel Core i5, Memory 4GB). We run the algorithms for 1000 realizations of the network and compute the running time in ms as shown in Table 1. We observe that the STSL and the GN-JSL respectively have the least and the second least average computational time with 0.15 ms and 0.67 ms while the JSL holds the highest one with 97.7 ms. To explain this, the JSL includes two bisection search in each iteration for the compensation of stratification effect, which is the most complex part of the algorithm. In order to have a higher accuracy, the bisection search needs more steps. Although GN-JSL has slightly higher complexity than the STSL, the localization performance of GN-JSL has been greatly improved which will be shown in the following section.

TABLE 1. Average computational time of the considered algorithms.

Algorithm	Time (ms)
JSL in [28]	97.70
STSL in [27]	0.15
GN-JSL	0.67

V. PERFORMANCE EVALUATIONS

In this section, extensive MATLAB simulations are conducted to evaluate the performance of the GN-JSL algorithm. The simulation parameters are described firstly. Then the metrics used to evaluate the performance of the considered algorithms are introduced. Finally, the synchronization accuracy, localization accuracy and energy consumption of the GN-JSL algorithm are compared with that of the JSL and STSL algorithms.

A. SIMULATION SETUP

We consider an UWSNs, in which 8 anchors are located on the vertices of a cube with edge length 2000 m and 1 ordinary node is located d meters away from the cube's center of gravity, where d has a normal distribution with zero mean and stand deviation of 100 m. The geometry of the ordinary node and anchor node locations is shown in Fig. 4. The clock skew is drawn from the i.i.d Gaussian random variables with mean 10^4 ppm and variance 10^6 ppm^2. The clock offset is drawn from the i.i.d Gaussian random variables with mean 1 s and variance 0.1 s^2. We assume that the sound propagation speed at $z = 0$, i.e. the surface, is $b = 1420$ m/s, and it increases as a linear function of depth with a steepness of $a = 0.01$. The number of one-way message exchange is set to 20. Unless specified otherwise, we have the simulation parameters listed in Table 2. For the sake of comparison, we also consider the STSL method and JSL method because both of them are joint synchronization and localization schemes for UWSNs proposed recently. Performance of these algorithms are compared in terms of synchronization accuracy, localization accuracy and energy efficiency. We evaluate several parameters which affect these algorithms, such as the propagation delay measurement noise, the steepness of SSP, the number of messages, and the number of reference nodes. We conduct Monte Carlo (MC) simulations, all simulation results are averaged of $N_{mc} = 2000$ independent runs.

TABLE 2. Simulation parameters.

Prameter	Value
Deployment region	$2000m \times 2000m \times 2000m$
Reference node number	8
Ordinary node number	1
Standard deviation of d	100 m
Clock skew	$\mathcal{N}(10^4 ppm, 10^6 ppm^2)$
Clock offset	$\mathcal{N}(1s, 0.1s^2)$
SSP	$a = 0.01s^{-1}, b = 1420ms^{-1}$
Number of messages	20
Simulation run	$N_{mc} = 2000$

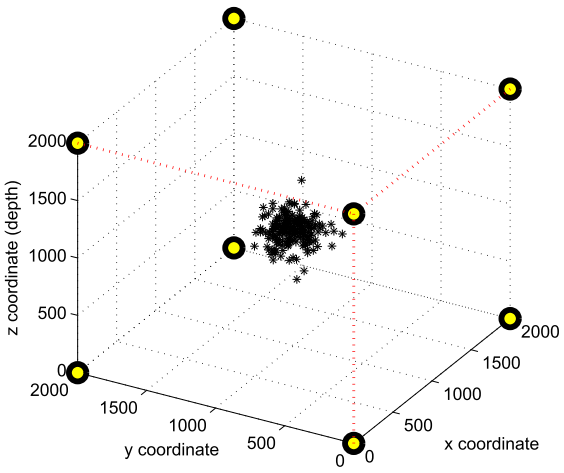

FIGURE 4. The geometry of the anchor nodes and the ordinary node locations.

B. METRICS

In this work, three metrics are used to evaluate the performance of the proposed algorithm. The first two metrics are the root mean square error (RMSE) of the ordinary node position $\mathbf{x}$ and the clock parameters $(\alpha, \beta)^T$ respectively, denoted by $RMSE_L$ and $RMSE_S$. They are defined as follows:

$$RMSE_L = \sqrt{\frac{\sum_{i=1}^{N_{mc}} ((x-\hat{x}_i)^2 + (y-\hat{y}_i)^2 + (z-\hat{z}_i)^2)}{N_{mc}}}, \quad (31)$$

$$RMSE_S = \sqrt{\frac{\sum_{i=1}^{N_{mc}} (\xi-\hat{\xi}_i)^2}{N_{mc}}}, \quad \xi = \alpha \text{ or } \beta, \ \hat{\xi}_i = \hat{\alpha}_i \text{ or } \hat{\beta}_i, \quad (32)$$

where $(\hat{x}_i, \hat{y}_i, \hat{z}_i)$ and $\hat{\xi}_i$ are the estimated coordinates and the clock parameters of the ordinary node at ith simulation run, respectively.

Another metric is energy efficiency, which is defined as:

$$\rho = \frac{t_{all}}{k_s n_m l_p}, \quad (33)$$

where k_s denotes the number of executions of a certain considered algorithm needed in the period of t_{all} seconds to keep the clock error below certain value. The term n_m represents the number of messages for each execution and l_p is packet size.

C. IMPACT OF MEASUREMENT NOISE ON ESTIMATION ERROR

We first investigate the RMSE performance of the considered algorithms versus average standard deviation of the measurement noise. Fig. 5 shows that all the performance of the considered algorithms become worse with an increasing standard deviation of the measurement noise. The proposed GN-JSL algorithm provides the optimal accuracy in both synchronization and localization, and its performance is close to the CRLB. It is also observed that the GN-JSL estimator starts to sperate from the CRLB for higher stand deviations of the noise. This is because that GN-JSL is a ML estimator which achieves the CRLB when the sample size tends to infinity or the measurement noise is very low. We note that although STSL performs better than JSL in synchronization, its localization performance is worse than JSL. This is mainly because of two reasons. First, the time synchronization and localization are performed at different phases in JSL, which is not a unified framework. Thus, the accuracy of the synchronization and localization are limited. Second, although STSL dose not consider the stratification effect, which reduces the accuracy of localization, the performance of synchronization is slightly affected by the stratification effect due to the two-way timing message signaling approach. In which, the propagation delay is considered as a constant, which is eliminated in the estimation process of clock parameters. We conclude that GN-JSL can significantly improve the accuracy of both synchronization and localization, which benefits from the unified framework design and the stratification compensation.

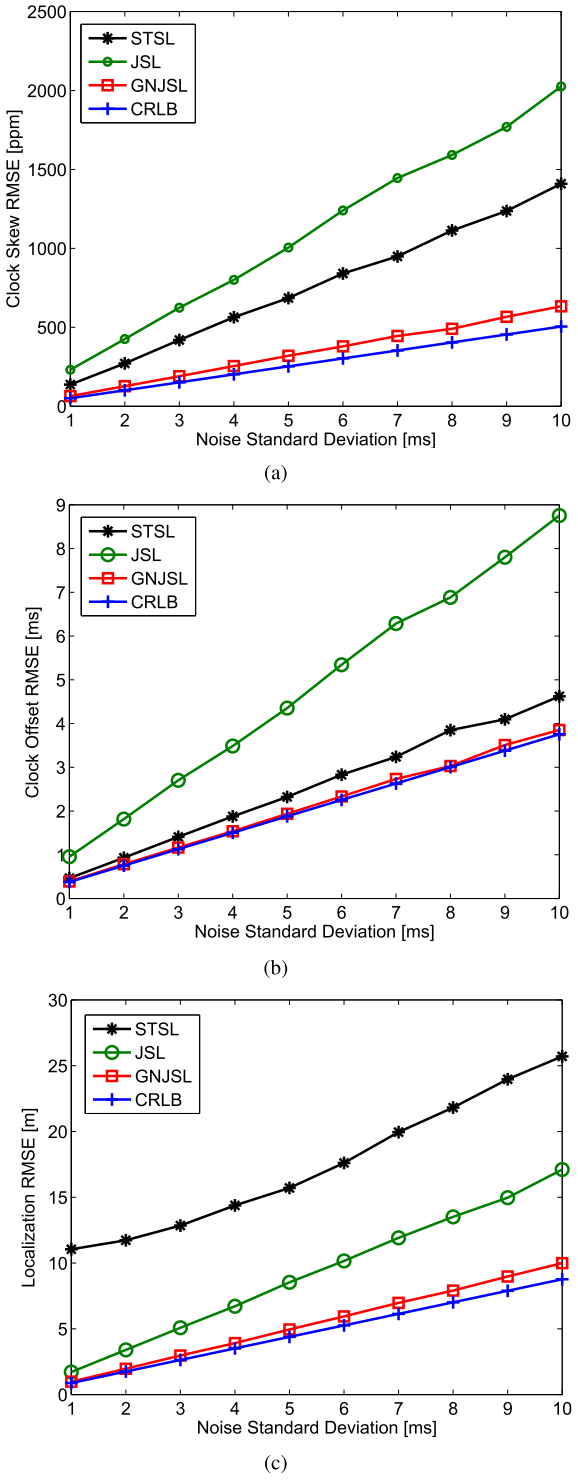

FIGURE 5. Impact of the measurement noise on RMSE performance of the considered algorithms: (a) clock skew; (b) clock offset; (c) location.

D. IMPACT OF STEEPNESS OF SSP ON ESTIMATION ERROR

Fig. 6 depicts the effect of the steepness of the SSP on the performance of the considered algorithms. As shown

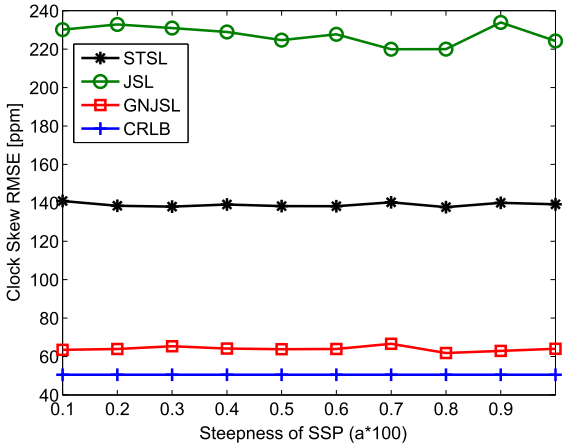

(a)

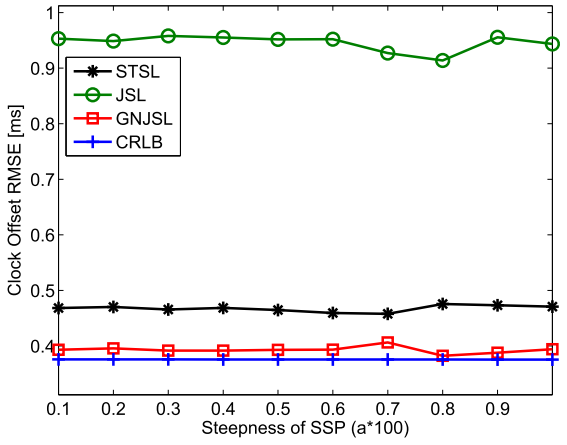

(b)

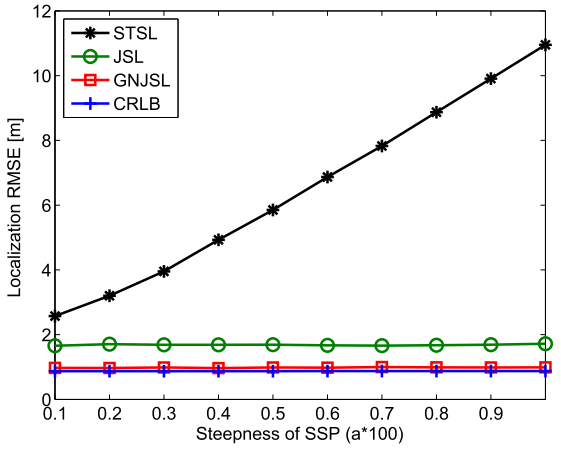

(c)

FIGURE 6. Impact of the steepness of SSP on RMSE performance of the considered algorithms: (a) clock skew; (b) clock offset; (c) location.

in Fig. 6(a) and Fig. 6(b), all of the considered algorithms are hardly affected by the steepness of the SSP and the GN-JSL holds the optimal accuracy in synchronization. This is because the synchronization phase in STSL and JSL is independent on the sound wave propagation path, and the propagation delay is regarded as an unknown constant. The gap between the STSL and JSL is mainly because the JSL dose not combine the synchronization and localization in a unified framework, which weakens the synchronization performance although the stratification effect is considered. Fig. 6(c) shows that the localization performance of the methods compensating for the stratification effect are hardly affected by the steepness of the SSP. The STSL without the stratification compensation suffers from significant location estimation errors, which indicates the importance of the stratification effect. Additionally, the GN-JSL performs much better than the other two methods in localization. Fig. 6 also shows that both the performance of synchronization and localization obtained by GN-JSL are quite close to the CRLB, which confirms the effectiveness of the unified framework design and the stratification compensation of the proposed method.

E. IMPACT OF NUMBER OF MESSAGES ON ESTIMATION ERROR

Fig. 7 demonstrates the impacts of the message overhead on the performance of considered algorithms. In this simulation, we run the algorithms with different number of messages, ranging from 18 to 60. The simulation results reveal that all the methods considered in this simulation achieve better synchronization accuracy when more message are exchanged. The reason for this phenomenon is that the more exchanged messages are involved, the more sample data can be used to conduct liner regression. Since both STSL and JSL exploit the liner regression to estimate the clock skew and clock offset, the accuracy of the synchronization of both methods benefit from the more exchanged messages. For GN-JSL, the improvement of the synchronization accuracy mainly benefits from the more precise estimate of the initial position when more exchanged messages are involved. However, the decreasing trend of the synchronization error of the GN-JSL method is more flat compared with STSL and JSL. In other words, the proposed GN-JSL method can achieve better synchronization accuracy with the same number of messages. In terms of localization, Fig. 7(c) shows that GN-JSL and JSL have better performance than the STSL. In addition, the localization performance of all the considered algorithms increase slightly as the number of exchanged messages increases. This is because ignoring the stratification effect would lead to a significantly bias in the range estimates, thus increasing the number of messages has very limited ability to enhance the localization performance. Compared to the synchronization performance, the localization performance is almost unaffected by the number of messages. This is mainly because the localization performance is dominated by the range estimates, which are not obtained directly from liner regression method. To this end, we conclude that an estimator which provides better accuracy in synchronization not necessarily to provide better performance in localization without the stratification compensation.

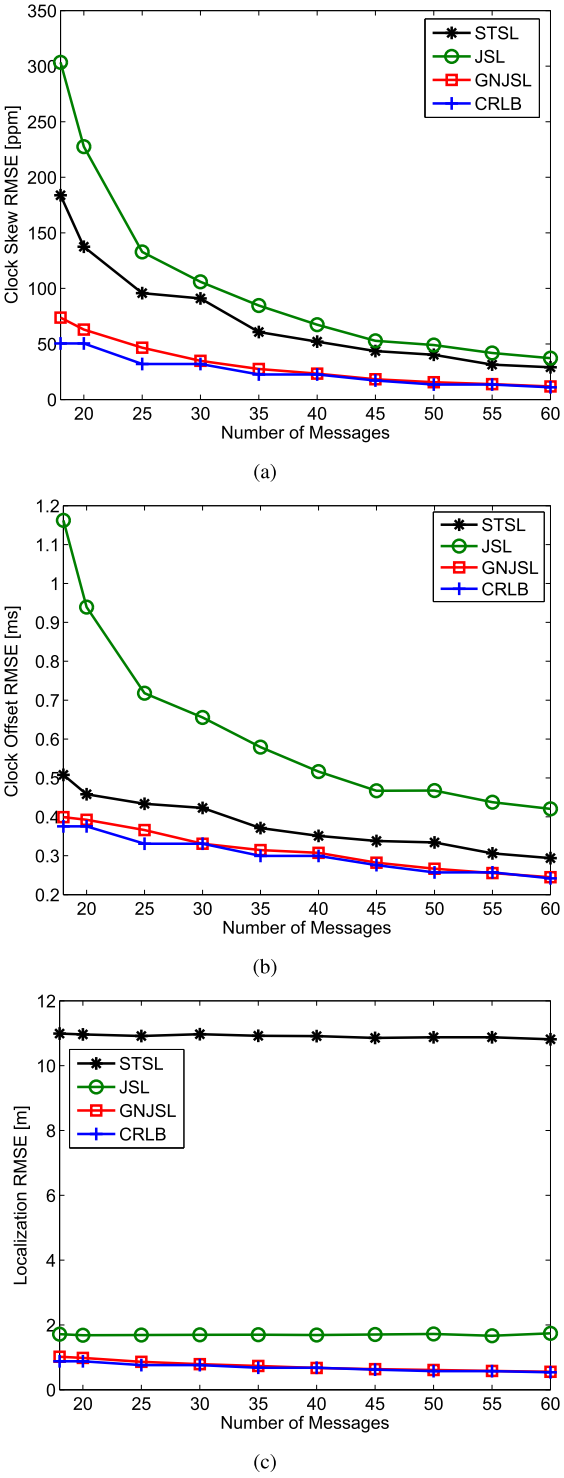

FIGURE 7. Impact of number of messages on RMSE performance of the considered algorithms: (a) clock skew; (b) clock offset; (c) location.

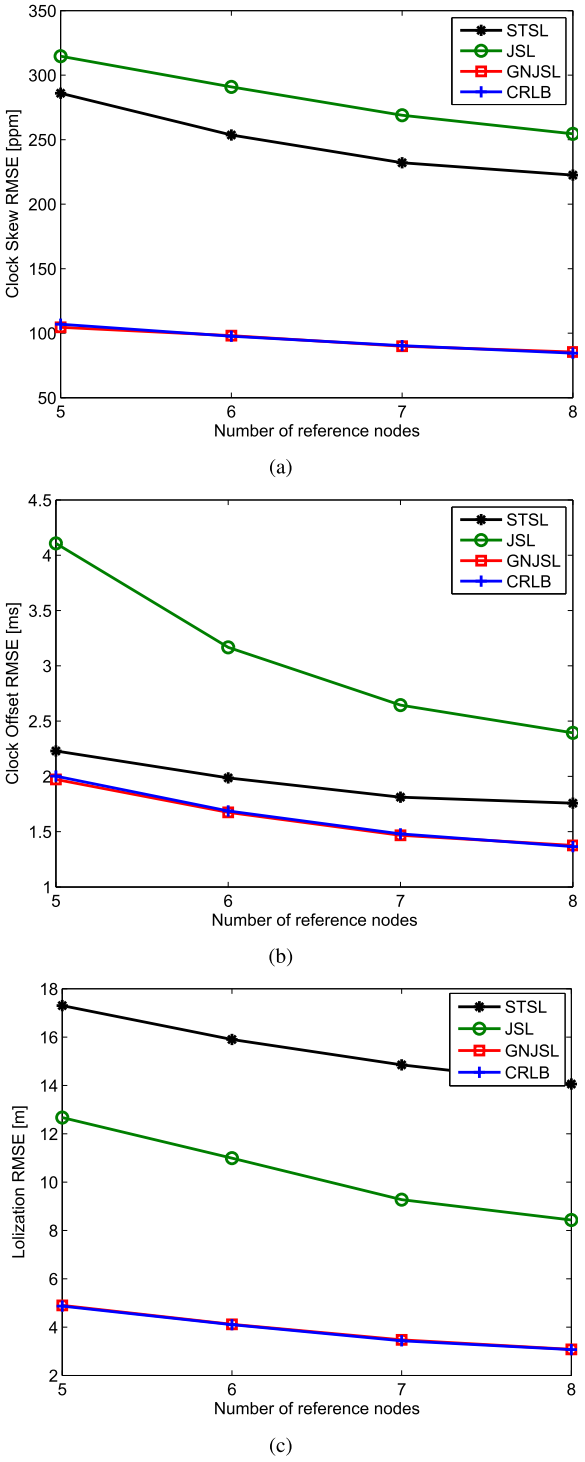

FIGURE 8. Impact of number of reference nodes on RMSE performance of the considered algorithms: (a) clock skew; (b) clock offset; (c) location.

F. IMPACT OF NUMBER OF REFERENCE NODES ON ESTIMATION ERROR

Fig. 8 shows the effect of the number of reference node on the RMSE performance of the considered algorithms. In this simulation, we fix the noise standard deviation as 5 ms. The anchors are added one by one and are located on the vertices of the cube as defined in Fig. 4. The number of message exchange between each pair of ordinary node and reference node is set to be 6. The results show that, for all considered algorithms, increasing the number of reference node improves both the performance of synchronization

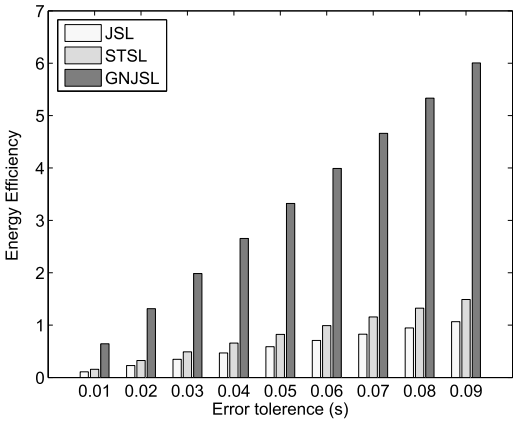

FIGURE 9. Energy efficiency with varying error tolerance.

and localization. Again, the RMSEs provided by GN-JSL are close to the CRLB and outperform the RMSEs obtained by STSL or JSL.

G. ENERGY EFFICIENCY

Since the available energy for sensor nodes in UWSNs is very limited, energy efficient is an important metric to evaluate the synchronization and localization algorithms. Different from the radio frequency (RF) communications, acoustic modems typically consume much more power in the transmit mode compared to the receive mode. On this basis, in GN-JSL, reference nodes broadcast one-way messages to synchronize and localize the ordinary node. Ordinary node is in receive mode, and it does not need to send messages. This makes the GN-JSL method to be an energy-efficient algorithm. The energy efficiency can be described by (33). In this simulation, we fix the number of messages n_m as 20, and t_{all} as 10^6 seconds for the considered algorithms. l_p is set to 40 Bytes for JSL and STSL both which employ two-way message signaling approach, and 25 Bytes for GN-JSL which employs one-way message signaling approach. Fig. 9 illustrates the energy efficiency of all the considered algorithms for error tolerance is changing from 0.01 s s to 0.09 s. It can be seen from the figure that the energy efficiency of all the methods increases as the tolerated error is relaxed. The reason is that, with a certain synchronization accuracy, the frequency of resynchronization decreases as the tolerated error increases. What's more, the results also show that GN-JSL has higher energy efficiency than the other two algorithms for all ranges of the tolerated error. The reason is that the GN-JSL has a higher synchronization accuracy compared to the other two algorithms, which leads to a smaller k_s. We can draw the conclusion that the proposed method can effectively reduce the message overhead, which is quite significant for UWSNs with limited energy capacity.

VI. CONCLUSIONS

The stratification effect in underwater environment degrades the performance of the straight-line propagation model based UWSNs synchronization and localization algorithms. Thus, in this paper, we present GN-JSL, a unified framework for time synchronization and localization. In GN-JSL, we apply the ray tracing method to model the stratification effect. In order to solve the synchronization and localization problems simultaneously, the stratification effect, clock imperfections, ordinary node location are formulated into a unified framework. The system model and its corresponding ML estimator are derived. Since the ML estimator is highly nonlinear and nonconvex, we employ the Gauss-Newton algorithm to solve the original problem with a rough estimated initial point. In addition, GN-JSL adopts the one-way message signaling approach to achieve high energy efficiency. Computer simulations are used to evaluate the performance of the proposed method. Simulation results show that GN-JSL can achieve higher synchronization accuracy, localization accuracy and energy efficiency compared with the previously joint estimators considered in the literature.

The proposed algorithm is designed to localize a single ordinary node. However, UWSNs are usually large-scale networks and the underwater acoustic communication range is limited by the energy constraints. This presents great difficulties and challenges to the localization of underwater nodes in large-scale UWSNs. Our future works include extending the proposed algorithm for localization in large-scale underwater networks. A good start point is to study the multi-stage scheme. In this scheme, the localized ordinary nodes can be used to help positioning other to-be-localized ordinary nodes. As this process iteratively performed, the localization coverage is expected to be increased.

REFERENCES

[1] J. Heidemann, M. Stojanovic, and M. Zorzi, "Underwater sensor networks: Applications, advances and challenges," *Philos. Trans. Roy. Soc. London A, Math. Phys. Sci.*, vol. 370, no. 1958, pp. 158–175, Jan. 2012.
[2] N. Mohamed, I. Jawhar, J. Al-Jaroodi, and L. Zhang, "Sensor network architectures for monitoring underwater pipelines," *Sensors*, vol. 11, no. 11, pp. 10738–10764, Nov. 2011.
[3] M. Stojanovic and J. Preisig, "Underwater acoustic communication channels: Propagation models and statistical characterization," *IEEE Commun. Mag.*, vol. 47, no. 1, pp. 84–89, Jan. 2009.
[4] P. Qarabaqi and M. Stojanovic, "Statistical characterization and computationally efficient modeling of a class of underwater acoustic communication channels," *IEEE J. Ocean. Eng.*, vol. 38, no. 4, pp. 701–717, Oct. 2013.
[5] I.-K. Rhee, J. Lee, J. Kim, E. Serpedin, and Y.-C. Wu, "Clock synchronization in wireless sensor networks: An overview," *Sensors*, vol. 9, no. 1, pp. 56–85, 2009.
[6] Y.-C. Wu, Q. Chaudhari, and E. Serpedin, "Clock synchronization of wireless sensor networks," *IEEE Signal Process. Mag.*, vol. 28, no. 1, pp. 124–138, Jan. 2011.
[7] J. Zheng and Y.-C. Wu, "Joint time synchronization and localization of an unknown node in wireless sensor networks," *IEEE Trans. Signal Process.*, vol. 58, no. 3, pp. 1309–1320, Mar. 2010.
[8] K. V. Mackenzie, "Nine-term equation for sound speed in the oceans," *J. Acoust. Soc. Amer.*, vol. 70, no. 3, pp. 807–812, Sep. 1981.
[9] C. R. Berger, S. Zhou, P. Willett, and L. Liu, "Stratification effect compensation for improved underwater acoustic ranging," *IEEE Trans. Signal Process.*, vol. 56, no. 8, pp. 3779–3783, Aug. 2008.
[10] M. B. Porter, "Acoustic models and sonar systems," *IEEE J. Ocean. Eng.*, vol. 18, no. 4, pp. 425–437, Oct. 1993.
[11] X. Wang, D. Jeske, and E. Serpedin, "An overview of a class of clock synchronization algorithms for wireless sensor networks: A statistical signal processing perspective," *Algorithms*, vol. 8, no. 3, pp. 590–620, Aug. 2015.

[12] J. Elson, L. Girod, and D. Estrin, "Fine-grained network time synchronization using reference broadcasts," in *Proc. OSDI*, Boston, MA, USA, Dec. 2002, pp. 147–163.
[13] S. Ganeriwal, R. Kumar, and M. B. Srivastava, "Timing-Sync protocol for sensor networks," in *Proc. SenSys*, Los Angeles, CA, USA, Nov. 2003, pp. 138–149.
[14] J. van Greunen and J. Rabaey, "Lightweight time synchronization for sensor networks," in *Proc. WSNA*, San Diego, CA, USA, Sep. 2003, pp. 11–19.
[15] M. Maróti, B. Kusy, G. Simon, and A. Lédeczi, "The flooding time synchronization protocol," in *Proc. SenSys*, Baltimore, MD, USA, Nov. 2004, pp. 39–49.
[16] A. A. Syed and J. Heidemann, "Time synchronization for high latency acoustic networks," in *Proc. INFOCOM*, Barcelona, Spain, Apr. 2006, pp. 1–12.
[17] N. Chirdchoo, W.-S. Soh, and K. C. Chua, "MU-Sync: A time synchronization protocol for underwater mobile networks," in *Proc. WuWNeT*, San Francisco, CA, USA, Sep. 2008, pp. 35–42.
[18] F. Lu, D. Mirza, and C. Schurgers, "D-Sync: Doppler-based time synchronization for mobile underwater sensor networks," in *Proc. WUWNet*, Woods Hole, MA, USA, Sep. 2010, pp. 1–8.
[19] J. Liu, Z. Zhou, Z. Peng, and J. H. Cui, "Mobi-Sync: Efficient time synchronization for mobile underwater sensor networks," in *Proc. GLOBECOM*, Miami, FL, USA, Dec. 2010, pp. 1–5.
[20] J. Liu, Z. Wang, M. Zuba, Z. Peng, J.-H. Cui, and S. Zhou, "DA-Sync: A Doppler-assisted time-synchronization scheme for mobile underwater sensor networks," *IEEE Trans. Mobile Comput.*, vol. 13, no. 3, pp. 582–595, Mar. 2014.
[21] G. Han, J. Jiang, L. Shu, Y. Xu, and F. Wang, "Localization algorithms of underwater wireless sensor networks: A survey," *Sensors*, vol. 12, no. 2, pp. 2026–2061, 2012.
[22] K. Y. Foo and P. Atkins, "A relative-localization algorithm using incomplete pairwise distance measurements for underwater applications," *Eurasip J. Adv. Signal Process.*, vol. 2010, no. 1, p. 930327, Dec. 2010.
[23] G. Casalino, A. Turetta, E. Simetti, and A. Caiti, "RT^2: A real-time ray-tracing method for acoustic distance evaluations among cooperating AUVs," in *Proc. OCEANS*, Sydney, Australia, May 2010, pp. 1–8.
[24] P. M. Ameer and L. Jacob, "Localization using ray tracing for underwater acoustic sensor networks," *IEEE Commun. Lett.*, vol. 14, no. 10, pp. 930–932, Oct. 2010.
[25] H. Ramezani, H. Jamali-Rad, and G. Leus, "Target localization and tracking for an isogradient sound speed profile," *IEEE Trans. Signal Process.*, vol. 61, no. 6, pp. 1434–1446, Mar. 2013.
[26] C. Tian, W. Liu, J. Jin, Y. Wang, and Y. Mo, "Localization and synchronization for 3D underwater acoustic sensor networks," in *Proc. UIC*, Hong Kong, Jul. 2007, pp. 622–631.
[27] R. Diamant and L. Lampe, "Underwater localization with time-synchronization and propagation speed uncertainties," *IEEE Trans. Mobile Comput.*, vol. 12, no. 7, pp. 1257–1269, Jul. 2013.
[28] J. Liu, Z. Wang, J.-H. Cui, S. Zhou, and B. Yang, "A joint time synchronization and localization design for mobile underwater sensor networks," *IEEE Trans. Mobile Comput.*, vol. 15, no. 3, pp. 530–543, Mar. 2016.
[29] S. M. Kay, *Fundamentals of Statistical Signal Processing, Estimation Theory*. Upper Saddle River, NJ, USA: Prentice-Hall, 1993.
[30] M. R. Gholami, S. Gezici, and E. G. Strom, "TDOA based positioning in the presence of unknown clock skew," *IEEE Trans. Commun.*, vol. 61, no. 6, pp. 2522–2534, Jun. 2013.

BINGBING ZHANG received the B.S. degree in electronic engineering and the M.S. degree in electronic science and technology from the National University of Defense Technology, Changsha, China, in 2011 and 2013, respectively, where he is currently pursuing the Ph.D. degree with the School of Electronic Science. From 2016 to 2017, he visited the Department of Automation, Shanghai Jiao Tong University, China. His main research interests lie in the areas of underwater localization, navigation, and target tracking.

HONGYI WANG received the B.S. degree from the Beijing University of Aeronautics and Astronautics, Beijing, China, in 2001, and the M.S. and Ph.D. degrees in electronic engineering from the National University of Defense Technology, Changsha, China, in 2003 and 2008, respectively. He is currently an Assistant Professor with the ASIC Research and Development Center, National University of Defense Technology. His research interests include digital design, wireless system design, and test and debug.

LIMING ZHENG received the M.S. degree in control engineering and the Ph.D. degree in computer science from the National University of Defense Technology, Changsha, China, in 2007 and 2012, respectively. He is currently an Associate Professor with the School of Electronic Science and Engineering, National University of Defense Technology. His research interests include network and information security, Internet of Things, and mobile ad hoc networks.

JIANFEI WU received the M.S. and Ph.D. degrees in electrical science and engineering from the National University of Defense Technology, Changsha, China, in 2008 and 2013, respectively. His current research interests include electromagnetic compatibility testing, modeling, and the simulation of analog IC circuits.

ZHAOWEN ZHUANG received the B.S. and M.S. degrees from the National University of Defense Technology (NUDT), Changsha, China, in 1981 and 1984, and the Ph.D. degree from the Beijing Institute of Technology, Beijing, China, in 1989. He is currently a Professor and the Deputy Head of NUDT. His research interests lie in the area of artificial intelligence and target recognition.